Journal of Alloys and Compounds 506 (2010) 22–26

Contents lists available at ScienceDirect

Journal of Alloys and Compounds

journal homepage: www.elsevier.com/locate/jallcom

Prediction study of the axial compressibility, anisotropy and dynamic properties for single crystal Ti_2GeC

Hongzhi Fu[a,b,*], WenFang Liu[c], Yanming Ma[c,*], Tao Gao[d]

[a] College of Physics and Electronic Information, Luoyang Normal College, Luoyang 471022, People's Republic of China
[b] National Laboratory of Superhard Materials, Jilin University, Changchun 130012, People's Republic of China
[c] College of Chemistry and Chemical Engineering, Luoyang Normal College, Luoyang 471022, People's Republic of China
[d] Institute of Atomic and Molecular Physics, Sichuan University, Chengdu 610065, People's Republic of China

ARTICLE INFO

Article history:
Received 23 March 2010
Received in revised form 28 June 2010
Accepted 30 June 2010
Available online 8 July 2010

PACS:
62.20.de
65.40.-b
71.15.Mb

Keywords:
Ti_2GeC
Elastic properties
Thermodynamic properties
Ab initio calculations

ABSTRACT

A theoretical formalism is used to study Ti_2GeC the compressibility, anisotropy and thermodynamic properties under pressure. The bulk moduli along the a and c axes, B_a and B_c, almost linearly increase with pressure, and the former is always smaller than the latter. The value of B_c/B_a has a trend of gradual increase as the pressure increases. It is found that the elastic constants, anisotropies and Debye temperature of Ti_2GeC increase monotonically with pressure. The thermal properties including the equation of state, hermal expansion coefficient α, the Grüneisen parameter γ, the anisotropies Δ_p, Δ_{S1} and Δ_{S2}, at various pressures and temperatures are estimated.

1. Introduction

The MAX compounds exhibit the favorable properties of ceramics and metals [1–8] where M is an early transition element, A is an A-group element (mostly IIIA and IVA element) and X is either C or N. This family of these compounds exhibit hexagonal crystal symmetry, with the general chemical formula $M_{n+1}AX_n$, where n varies from 1 to 3. Based on the value of n, this class of materials can be further classified as M_2AX or 211MAX compounds ($n=1$), M_3AX_2 or 312 MAX compounds ($n=2$) and M_4AX_3 or 413 MAX compounds ($n=3$). More than 50 compounds of the so-called M_2AX phases are reported. These compounds are layered with two formula units per unit cell. With the hexagonal structure, Ti_2GeC shows a large c/a ratio because the unit cell is very large in c axis as compared to a axis, almost three times. The atoms therefore have more freedom to move and rearrange in c direction than in a direction. Moreover, the symmetry restrictions allow only the z co-ordinate of Ti to be at general position.

Recently, Phatak et al. reported on the synthesis and compressibility of Ti_2GeC, Ti_2AlC and Ti_2SC [9]. Ti_2AlC has been widely studied owing to one of the lowest density among all the 211 MAX compounds so far [10,11]. More recently Ti_2SC has been synthesized [12] and its high-pressure behavior [13] has been reported.

From above, it is clear that some fundamental properties of Ti_2GeC have been not investigated compared to the other members of this family. Few experimental and theoretical works have been done to investigate their properties. In this paper we study Ti_2GeC compressibility, anisotropy and thermodynamic properties under higher pressure. These properties are important not only because they are closely related to various fundamental solid-state phenomena such as interatomic bonding, equations of state, and phonon spectra, but also they link thermodynamically with the specific heat, thermal expansion, Debye temperature, melting point, and Grüneisen parameter. The effects of pressure are considered here because they have already displayed much marvellous physics phenomenon recently [14]. The motivations are to study the elastic and thermal behavior of Ti_2GeC and to investigate if it exhibits any unusual behavior under high pressure.

2. Computational details

All calculations are performed based on the plane-wave pseudopotential density function theory (DFT) [15,16]. Vanderbilt-type

* Corresponding authors at: College of Physics and Electronic Information, Luoyang Normal College, Luoyang 471022, People's Republic of China.
Tel.: +86 0379 65515016; fax: +86 0379 65515016.
E-mail address: fhzscdx@163.com (H. Fu).

0925-8388/$ – see front matter © 2010 Elsevier B.V. All rights reserved.
doi:10.1016/j.jallcom.2010.06.186

Table 1
Unit cell parameters, molar volume and their relative lattice parameters at different pressures for Ti_2GeC.

Pressure (GPa)	a (Å)	c (Å)	V (Å^3)	a/a_0	c/c_0	V/V_0
Present						
0	3.101	13.159	109.61	1	1	1
5	3.065	13.024	106.02	0.988	0.989	0.967
10	3.035	12.909	103.00	0.978	0.980	0.939
15	3.008	12.813	100.46	0.970	0.973	0.916
20	2.984	12.720	98.13	0.962	0.966	0.895
25	2.962	12.633	96.03	0.955	0.959	0.876
30	2.942	12.561	94.17	0.948	0.954	0.859
35	2.923	12.490	92.47	0.942	0.949	0.843
40	2.906	12.427	90.94	0.937	0.944	0.829
45	2.890	12.367	89.46	0.931	0.939	0.816
50	2.874	12.314	88.11	0.926	0.935	0.803
55	2.859	12.262	86.86	0.922	0.931	0.792
60	2.845	12.215	85.67	0.917	0.928	0.781
65	2.812	12.117	83.01	0.906	0.9208	0.757
70	2.800	12.078	82.01	0.902	0.917	0.748
Experiment [9]						
0	3.078	12.934	106.13	1.000	1.000	1.000
1.35	3.073	12.896	105.48	0.998	0.997	0.994
3.35	3.066	12.856	104.64	0.996	0.994	0.986
4.19	3.061	12.843	104.22	0.994	0.993	0.982
5.72	3.056	12.799	103.53	0.993	0.990	0.975
8.12	3.048	12.761	102.65	0.990	0.987	0.967
11.29	3.032	12.680	100.96	0.985	0.980	0.951
12.45	3.027	12.636	100.23	0.983	0.977	0.944
17.02	3.014	12.571	98.91	0.979	0.972	0.932
22.97	2.994	12.494	96.97	0.973	0.966	0.914
30.04	2.976	12.379	94.92	0.967	0.957	0.894
32.26	2.966	12.359	94.16	0.964	0.956	0.887
39.73	2.945	12.239	91.93	0.957	0.946	0.866
41.76	2.941	12.230	91.62	0.955	0.946	0.863
49.47	2.922	12.135	89.71	0.949	0.938	0.845

ultrasoft pseudopotentials (USPP) [17] are employed to describe the electron–ion interactions. The effects of exchange correlation interaction are treated with the generalized gradient approximation (GGA) of Perdew–Burke–Eruzerhof (PBE) [18]. In the structure calculation, a plane-wave basis set with energy cut-off 350.00 eV is used. Pseudo-atomic calculations are performed for $Ti3d^24s^2$, $Ge4s^24p^2$ and $C2s^22p^2$. For the Brillouin-zone sampling, we adopt the $9 \times 9 \times 2$ Monkhorst–Pack mesh [19], where the self-consistent convergence of the total energy is at 10^{-7} eV/atom and the maximum force on the atom is blow 10^{-5} eV/Å.

3. Results and discussions

The equilibrium lattice constant a, c, volume V and their ratios are listed in Table 1 with experiment results. It can found that our calculated values are consistent with the experiment data [9] at different pressures. For Ti_2GeC, there are five independent elastic constants, i.e., C_{11}, C_{12}, C_{13}, C_{33} and C_{44}. The complete elastic constant tensor was determined from calculations of the stresses induced by small deformations of the equilibrium primitive cell, and thus the elastic constants C_{ijkl} are determined as [20]

$$c_{ijkl} = \left(\frac{\partial \sigma_{ij}(x)}{\partial e_{kl}}\right)_X \tag{1}$$

where σ_{ij} and e_{kl} are applied stress and Eulerian strain tensors, and X and x are the coordinates before and after the deformation. For the isotropic stress, the elastic constants are defined as [21]

$$c_{ijkl} = C_{ijkl} + \frac{P}{2}(2\delta_{ij}\delta_{kl} - \delta_{il}\delta_{jk} - \delta_{ik}\delta_{jl}) \tag{2}$$

$$C_{ijkl} = \left(\frac{1}{V(x)}\frac{\partial^2 E(x)}{\partial e_{ij} e_{kl}}\right)_X \tag{3}$$

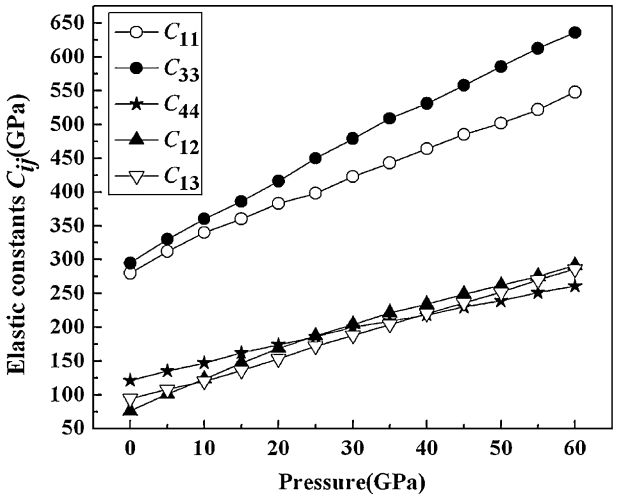

Fig. 1. The elastic constants C_{ij} of Ti_2GeC as a function of pressure, neglecting zero-point vibrational effects.

where C_{ijkl} are the second-order derivatives with respect to the infinitesimal strain.

Fig. 1 shows the elastic constants C_{ij} variation versus pressure (up to 60 GPa). We found that the five independent elastic constants increase monotonically with pressure. C_{33} and C_{12} vary rapidly as pressure increases, followed by C_{13}, C_{11} and C_{44}. Unfortunately, there are no experimental and theoretical data to compare our elastic constants under pressure. If this structure is stable, the five independent elastic constants should satisfy the well-known Born stability criteria [22], i.e.

$$C_{12} > 0, \quad C_{33} > 0, \quad C_{66} = (C_{11} - C_{12})/2 > 0, \quad C_{44} > 0, \tag{4}$$

and

$$(C_{11} + C_{12})C_{33} - 2C_{13}^2 > 0. \tag{5}$$

This suggests that the Ti_2GeC is mechanically stable and predicts that there is not a transition phase when the pressure is under 60 GPa.

The mechanical anisotropy of Ti_2GeC can be calculated using the bulk moduli along the a and c axes, B_a and B_c, respectively [23],

$$B_a = a\frac{dP}{da} = \frac{\Lambda}{2+\alpha} \tag{6}$$

$$B_c = c\frac{dP}{dc} = \frac{B_a}{\alpha}, \tag{7}$$

$$\Lambda = 2(C_{11} + C_{12}) + 4C_{13}\alpha + C_{33}\alpha^2, \tag{8}$$

$$\alpha = \frac{C_{11} + C_{12} - 2C_{13}}{C_{33} - C_{13}} \tag{9}$$

The calculated B_a and B_c with pressure are presented in Fig. 2. It can be seen that B_a and B_c almost linearly increase with pressure, and the former is always smaller than the latter. It is interesting that the value of B_c/B_a has a trend of gradual increase as the pressure increases. This may show that the mechanical behavior of Ti_2GeC under pressure is of anisotropy.

It is known that the acoustic velocities are obtained from elastic constants by the Christoffel equation [24]

$$(C_{ijkl}n_j n_k - M\delta_{il})\mu_i = 0 \tag{10}$$

where $M = \rho v^2$, C_{ijkl} is the fourth rank tensor description of the elastic constants, n is the propagation direction, and μ is the polarization vector; the acoustic anisotropy is defined as [25]

$$\Delta_i = \frac{M_i[n_x]}{M_i[100]} \tag{11}$$

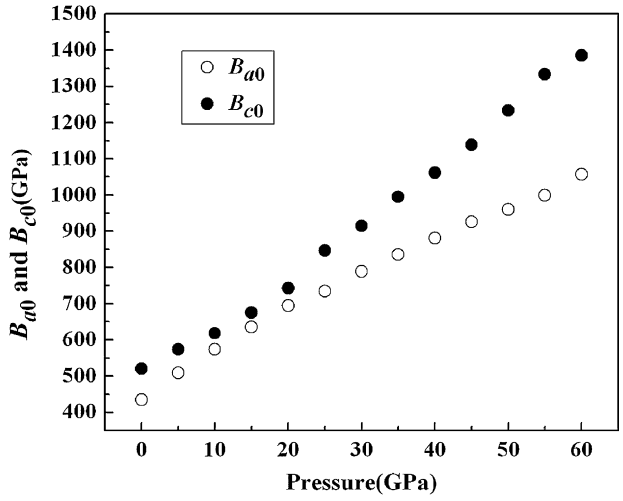

Fig. 2. Variation of the bulk modulus B_a and B_c along the *a*- and *c*-axes with pressure.

where n_x is the extremal propagation direction and i is the index of three types of elastic waves (one longitudinal and two traversal polarizations of shear waves). By solving the Christoffel equation (11) for hexagonal Ti_2GeC, the anisotropy of the compression wave is obtained from [26]

$$\Delta_p = \frac{V_l^2(0^0)}{V_l^2(90^0)} = \frac{C_{33}}{C_{11}} \tag{12}$$

The anisotropies of the wave polarized perpendicular to the basal plane ($S1$) and to the basal plane ($S2$) are calculated [26]

$$\Delta_{S1} = \frac{C_{11}+C_{33}-2C_{13}}{4C_{44}}, \quad \Delta_{S2} = \frac{V_t^2(0^0)}{V_t^2(90^0)} = \frac{2C_{44}}{C_{11}-C_{12}} \tag{13}$$

where Δ_p shows the anisotropy of the compression wave, Δ_{S1} and Δ_{S2} denote the shear waves, $V(90^0)$ and $V(0^0)$ are the in-plane and *c*-axis ultrasound velocities, respectively. For an elastically isotropic solid, $\Delta_p = \Delta_{S1} = \Delta_{S2} = 1$. The elastic anisotropy factors of Ti_2GeC are $\Delta_p = 1.05$, $\Delta_{S1} = 0.8$ and $\Delta_{S2} = 1.19$. This small anisotropy indicates that the in-plane and out-of-plane interatomic interactions in Ti_2GeC differ slightly. Fig. 3 shows the pressure dependences of the elastic anisotropy factors for Ti_2GeC in the range 0–60 GPa. It is noted that Δ_{S2} increases rapidly and Δ_p slightly with increasing pressure. However, Δ_{S1} decreases with pressure (due to the fact that the elastic constants C_{11} and C_{33} are affected by pressure). These are due to the anharmonicity of acoustic vibrations.

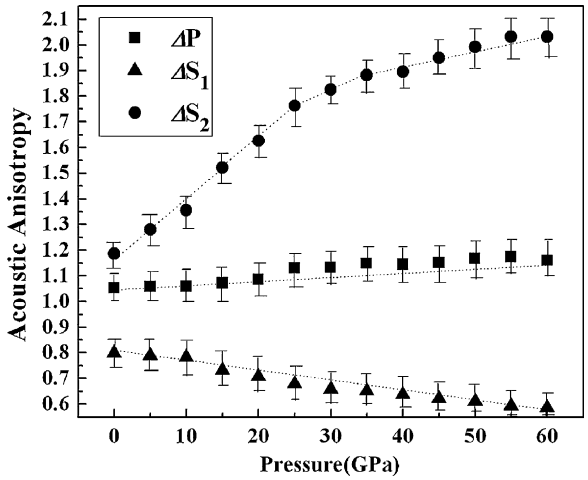

Fig. 3. Temperature dependences of the longitudinal and transverse elastic anisotropy factors for Ti_2GeC single crystals.

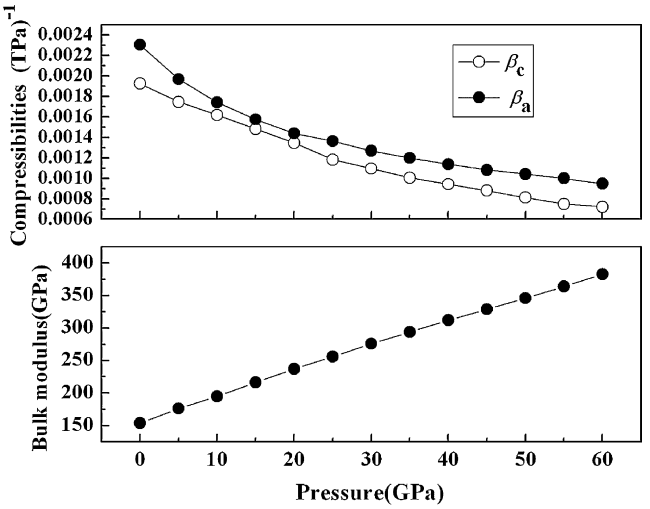

Fig. 4. Pressure dependence of the bulk modulus and *a* and *c* axis compressibilities of Ti_2GeC.

Isothermal compressibility measurements provide information about the nature of chemical bonding in crystals and make it possible to evaluate the Debye characteristic temperature, the difference between the heat capacities at constant pressure and volume, and other thermal parameters. The compressibility of semiconductors is difficult to determine by direct measurements and is commonly evaluated from elastic constants. The expression for compressibility β for the hexagonal and rhombohedral systems can be written in matrix notation as [27]

$$\beta = (S_{11}+S_{12}+S_{13}) - (S_{11}+S_{12}-S_{13}-S_{33})l^2 \tag{14}$$

where l is the direction cosine with the c axis ($l^2 = 0$ for $\perp c$ axis; $l^2 = 1$ for $\|c$ axis), S_{ij} the elastic-compliance-constant. Thus, the linear compressibility in the uniaxial materials is rotationally symmetrical about the unique axis *c*. The pressure dependence of the lattice parameter is also related to a combination of elastic constants C_{ij}, and thus we can make use of the linear compressibility β to check the validity of the calculated S_{ij}. In hexagonal crystal, the axial compressibilities β_a and β_c are of the form [28,29]

$$\beta_a = -d\ln a/dP = \frac{C_{33}-C_{13}}{\Omega}, \quad \beta_c = -d\ln c/dP = \frac{C_{11}+C_{12}-2C_{13}}{\Omega} \tag{15}$$

where $\Omega = (C_{11}+C_{12})C_{33} - 2C_{13}^2$

Here the β_a and β_c are of the linear compressibility. The volume compressibility of hexagonal layered crystals is $\beta = \beta_c + 2\beta_a$, where β_c and β_a are the *c*-axis and in-plane isothermal compressibilities, respectively. On the other hand, we can determine β_a and β_c by fitting a polynomial to the evolution of $\ln a$ and $\ln c$ at various pressures. The pressure effects on the axial compressibilities β_a and β_c are shown in Fig. 4. Our calculated β_a and β_c are equal to 0.0023 and 0.002 TPa^{-1}, respectively. As expected, compressibilities along the *a* and *c* axis decrease linearly with pressure while the bulk modulus increases, which accords with experiment [9].

The anisotropy of the crystal is measured by A_- and A_+ coefficient calculated for every symmetry plane and axis. These factors are derived from elastic constants by the following simple relationships [30]:

$$A_-^{[0\ 0\ 1]} = \frac{C_{44}(C_{11}+2C_{13}+C_{33})}{C_{11}C_{33}-C_{13}^2} \tag{16}$$

Table 2
Anisotropy factors A_-, A_+ for, respectively, symmetry plane (ijk) and $[ijk]$ symmetry axis with symmetry plane (ijk) as a function of pressure.

Pressure (GPa)	$A_-^{[001]}$	$A_+^{[100],(010)}$	$A_+^{[001],(010)}$
0	1.2516	−16.13333	1.20398
5	1.26873	−15	1.21622
10	1.27944	−14.7	1.225
15	1.36901	−12.46154	1.296
20	1.41459	−10.54545	1.32319
25	1.48286	−7.15385	1.33813
30	1.52804	−7.14286	1.37457
35	1.54587	−6.33333	1.37049
40	1.58008	−6.50746	1.40193
45	1.6212	−6.30137	1.42857
50	1.6495	−5.69048	1.43114
55	1.70153	−5.51648	1.46356
60	1.71826	−5.93182	1.49143

$$A_+^{[1\,00],(0\,1\,0)} = \frac{2C_{44}}{C_{11} - C_{33}} \tag{17}$$

$$A_+^{[0\,0\,1],(0\,1\,0)} = \frac{2C_{44}}{C_{33} - C_{13}} \tag{18}$$

The $[ijk]$ and (ijk) denote symmetry axis and plane, respectively. Anisotropy factors are easy to calculate and provide important in-plane phonon-focusing information. The three anisotropy factors provide the most useful information for hexagonal crystals. Positive values of A_+ less than unity indicate in-plane focusing, whereas values greater than unity indicate in-plane defocusing about the principal axis. For the rare case A_+ is negative. In-plane cuspidal features can be inferred from the values of A_-. Cuspidal features about a principal axis require A_- to be somewhat greater than unity [31]. The calculated anisotropy factors are presented in Table 2. One can note that Ti_2GeC shows anisotropy which coincides with the results of Scabarozi et al. [32]. And the anisotropy factors increase with pressure.

For Ti_2GeC crystal, the Debye temperature can be estimated from the average sound velocity V_m, using the following equation [33]

$$\theta = \frac{h}{k_B}\left(\frac{3nN_A\rho}{4\pi M}\right)^{1/3} V_m \tag{19}$$

where h is Planck's constant, k_B is Boltzmann's constant, N_A is Avogadro's number, M is the molecule mass, ρ is the density, and the average sound velocity V_m is approximately given by [34]

$$V_m = \left[\frac{1}{3}\left(\frac{2}{V_s^3} + \frac{1}{V_P^3}\right)\right]^{-(1/3)} \tag{20}$$

where V_p and V_s are the longitudinal and transverse elastic wave velocities, respectively, which can be obtained from Navier's equation [35]

$$V_p = \sqrt{\left(B_S + \frac{4}{3}G\right)/\rho}, \quad V_s = \sqrt{\frac{G}{\rho}} \tag{21}$$

where G is the shear modulus and B_S is the adiabatic bulk modulus.

The calculated values of θ_p/θ_0 are plotted in Fig. 5, where θ_0 is the Debye temperature at zero pressure, θ_p at pressure P. For Ti_2GeC, $\theta_p/\theta_0 > 1$, not like rubidium halides ($\theta_p/\theta_0 < 1$) [36]. There is qualitative agreement with the relation:

$$\theta_p = [1 + (\gamma\beta)P]\theta_0, \tag{22}$$

where γ is the Gruneisen constant and β the compressibility.

Fig. 6 shows the pressure dependence of the longitudinal wave (V_l) and transverse wave (V_t) velocities of Ti_2GeC. The V_l is always bigger than V_t, and they almost linearly increase with pressure. In this study the V_l at 0 GPa are 9.83 km/s and V_t 6.95 km/s, respectively. When the pressure reaches 60 GPa, V_l and V_t read 13.33 and 10.32 km/s, respectively. This shows that a slight wave velocities variation appears. We attribute this mostly to the changes in the shear modulus G and the bulk modulus B with pressure.

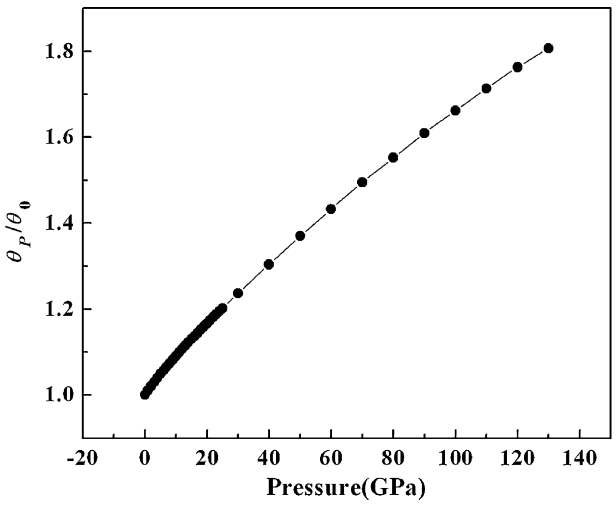

Fig. 5. θ_p/θ_0 obtained as a function of pressure P.

The thermal expansion coefficient α [37,38] is thought to be described the alteration in a frequency of the crystal lattice vibration based on the lattice's increase or decrease in volume as the temperature changes. It is directly related to the equation of state (EOS). We have determined the pressure dependence of the thermal expansion and that the results are shown in Fig. 7. It can be observed that the α increases monotonously when $T > 500$ K (as shown in Fig. 7a); while at fixed temperature, the α decreases dramatically with pressure (Fig. 7b). We can get the temperature dependence of thermal expansion coefficient α (10^{-5} K^{-1}) at different pressure.

$$\alpha(T) = 0.01031T - 2.42003 \times 10^{-5}T^2 + 2.92178 \times 10^{-8}T^3 - 1.87072 \times 10^{-11}T^4 + 6.08887 \times 10^{-15}T^5 - 7.91511 \times 10^{-19}T^6 \quad P = 0\,\text{GPa}$$

$$\alpha(T) = 0.00836T - 1.90242 \times 10^{-5}T^2 + 2.21221 \times 10^{-8}T^3 - 1.36309 \times 10^{-11}T^4 + 4.25162 \times 10^{-15}T^5 - 5.27725 \times 10^{-19}T^6 \quad P = 5\,\text{GPa}$$

$$\alpha(T) = 0.00718T - 1.57093 \times 10^{-5}T^2 + 1.73222 \times 10^{-8}T^3 - 1.00459 \times 10^{-11}T^4 + 2.91944 \times 10^{-15}T^5 - 3.33345 \times 10^{-19}T^6 \quad P = 10\,\text{GPa}$$

$$\alpha(T) = 0.00639T - 1.33826 \times 10^{-5}T^2 + 1.38772 \times 10^{-8}T^3 - 7.42032 \times 10^{-11}T^4 + 1.92761 \times 10^{-15}T^5 - 1.866 \times 10^{-19}T^6 \quad P = 15\,\text{GPa}$$

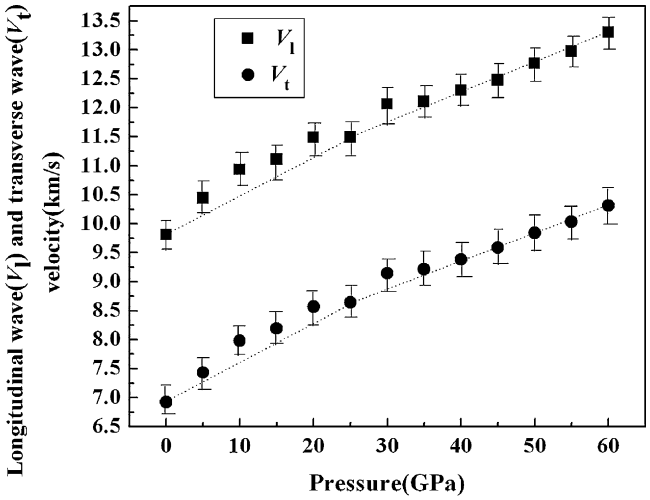

Fig. 6. The pressure dependence of longitudinal wave and transverse wave velocities of Ti_2GeC.

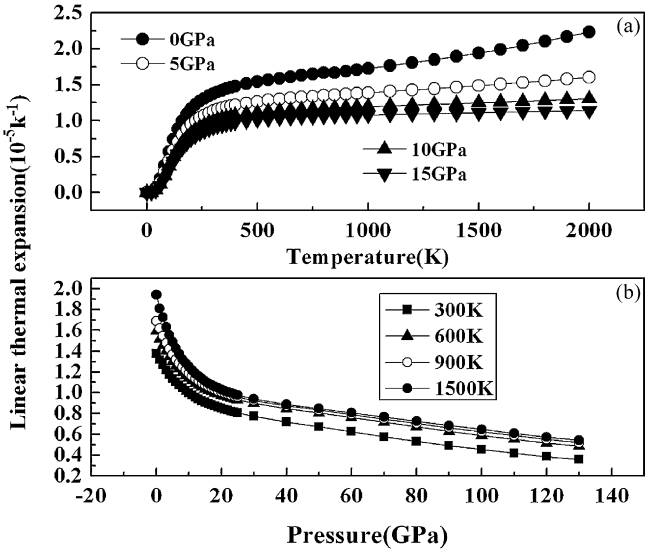

Fig. 7. Variation of the thermal expansion α with (a) temperature T and (b) pressure P.

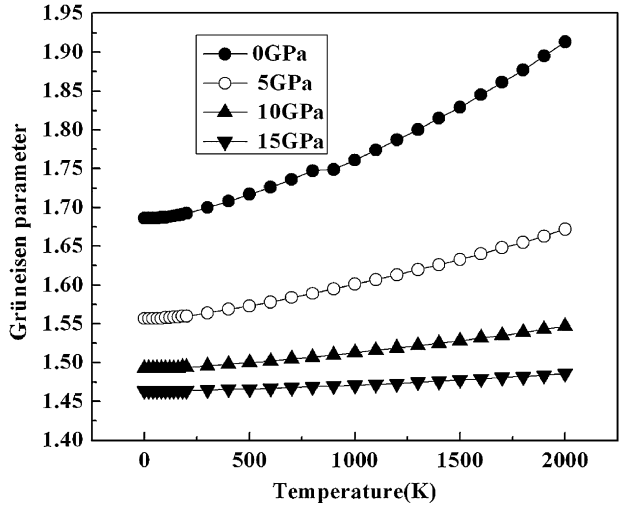

Fig. 8. Variation of the thermal expansion coefficient α with pressure P.

The dependence of the Grüneisen parameter γ [39] with pressure P are shown in Fig. 8. The effects of the pressure P on the Grüneisen parameter γ are obtained. However, it is noted that as the pressure increases, γ almost increases lineally. This means that there is a bigger thermal expansion at low pressure. The following relations are obtained, respectively.

$$\gamma(T) = 1.68338 + 4.60174 \times 10^{-5}T + 3.42574 \times 10^{-8}T^2 \quad P = 0\ \text{GPa}$$
$$\gamma(T) = 1.55458 + 3.2423 \times 10^{-5}T + 1.317 \times 10^{-8}T^2 \quad P = 5\ \text{GPa}$$
$$\gamma(T) = 1.49167 + 1.3974 \times 10^{-5}T + 6.90576 \times 10^{-9}T^2 \quad P = 10\ \text{GPa}$$
$$\gamma(T) = 1.4636 + 3.46025 \times 10^{-5}T + 3.86567 \times 10^{-9}T^2 \quad P = 15\ \text{GPa}$$

4. Conclusions

We have investigated the pressure-dependent elastic anisotropy, static compressibility and lattice dynamical properties of ternary alloy Ti_2GeC within the plane-wave pseudopotential density functional theory within the generalized gradient approximation method. The calculated lattice constants are in agreement with the experimental data. We have obtained the pressure dependence of thermal expansion coefficient α and Grüneisen parameter $\gamma(T)$. From the elastic constants, the bulk moduli along the crystallographic axes are calculated. It is found that its compressibility β and thermal expansion coefficient α decrease when increasing pressure; while the anisotropy factor, the c-axis and in-plane bulk moduli, Debye temperature, longitudinal wave and transverse wave velocities increase with pressure. The results are interpreted in terms of the anharmonicity of lattice vibrations, and the atomic bonding along the c-axis is stronger than that along the a-axis.

Acknowledgments

This project was supported by the National Natural Science Foundation of China under grant No. 40804034, and by the Natural Science Foundation of the Education Department of Henan Province of China under grant No. 2009B590001 and by Henan Science and Technology Agency of China under grant No. 092102210314.

References

[1] T. El-Raghy, M.W. Barsoum, S.R. Kalidindi, J. Am. Ceram. Soc. 82 (1999) 2849.
[2] M. Radovic, M.W. Barsoum, T.E. Raghy, S. Wiederhorn, W.E. Luecke, Acta Mater. 50 (2002) 1297.
[3] I. Salama, T. El-Raghy, M.W. Barsoum, J. Alloys Compd. 347 (1–2) (2002) 271.
[4] A. Ganguly, T. Zhen, M.W. Barsoum, J. Alloys Compd. 376 (1–2) (2004) 287.
[5] B. Cahn, F. Kramer, M. Veyssiere (Eds.), Encyclopedia of Materials Science & Technology, Elsevier Science, 2006.
[6] M. Radovic, M.W. Barsoum, A. Ganguly, T. Zhen, P. Finkel, S.R. Kalidindi, E. Lara-Curzio, Acta Mater. 54 (2006) 2757.
[7] J.D. Hettinger, S.E. Lofland, P. Finkel, T. Meehan, J. Palma, K. Harrell, S. Gupta, A. Ganguly, T. El-Raghy, M.W. Barsoum, Phys. Rev. B 72 (2005) 115120.
[8] M.W. Barsoum, I. Salama, T. El-Raghy, J. Golczewski, W.D. Porter, H. Wang, H.J. Seifert, F. Aldinger, Metall. Mater. Trans. 33a (2002) 2775.
[9] N.A. Phatak, S.K. Saxena, Y.w. Fei, J.z. Hu, J. Alloys Compd. 474 (2008) 174.
[10] A.G. Zhou, M.W. Barsoum, S. Basu, S.R. Kalidindi, T. El-Raghy, Acta Mater. 54 (2006) 1631.
[11] B. Manoun, F.X. Zhang, S.K. Saxena, M.W. Barsoum, T. El-Raghy, J. Phys. Chem. Solids 67 (9–10) (2006) 2091.
[12] S. Amini, M.W. Barsoum, T. El-Raghy, J. Am. Ceram. Soc. 90 (12) (2007) 3953.
[13] R. Shrinivas, R. Kulkarni, Selva Vennila, A. Nishad, S.K. Phatak, C.S. Saxena, T. Zha, M.W. El-Raghy, W. Barsoum, R. Luo, Ahuja, J. Alloys Compd. 448 (1–2) (2008) L1.
[14] Y.M. Ma, M. Eremets, A.R. Oganov, Y. Xie, I. Trojan, S. Medvedev, A.O. Lyakhov, M. Valle, V. Prakapenka, Nature 458 (2009) 182.
[15] P. Hohenberg, W. Kohn, Phys. Rev. B 136 (1964) 384.
[16] W. Kohn, L.J. Sham, Phys. Rev. A 140 (1965) 1133.
[17] D. Vanderbilt, Phys. Rev. B41 (1990) 7892.
[18] J.P. Perdew, K. Burke, M. Ernzerhof, Phys. Rev. Lett. 77 (1996) 3865.
[19] H.J. Monkhorst, J.D. Pack, Phys. Rev. B 13 (1976) 5188.
[20] B.B. Karki, G.J. Ackland, J. Crain, J. Phys.: Condens. Matter 9 (1997) 8579.
[21] D.C. Wallace, Thermodynamics of Crystals, Wiley, New York, 1972.
[22] M. Born, Proc. Cambridge Philos. Soc. 36 (1940) 160.
[23] A.K.M.A. Islam, A.S. Sikder, F.N. Islam, Phys. Lett. A 350 (2006) 288.
[24] M.A. Auld, Acoustic Fields and Waves in Solids, vol. 1, Wiley, New York, 1973.
[25] G.S. Neumann, L. Stixtude, R.E. Cohen, Phys. Rev. B 60 (1999) 791.
[26] G. Steinle-Neumann, L. Stixtude, R.E. Cohen, Phys. Rev. B 60 (1999) 791.
[27] D.B. Sirdeshmukh, L. Sirdeshmukh, K.G. Subhadra, A Handbook of Physical Properties, Springer-Verlag, Berlin, Heidelberg, New York, 2001.
[28] J.F. Nye, Physical Properties of Crystals: Their Representation by Tensors and Matrices, Clarendon, Oxford, 1985.
[29] T.H. Scabarozi, S. Amini, O. Leaffer, A. Ganguly, S. Gupta, W. Tambussi, S. Clipper, J.E. Spanier, M.W. Barsoum, J.D. Hettinger, S.E. Lofland, J. Appl. Phys. 105 (2009) 013543.
[30] K. Lau, A.K. McCurdy, Phys. Rev. B 58 (1998) 8980.
[31] D.C. Wallace, Thermodynamics of Crystals, Wiley, NY, 1972.
[32] T.H. Scabarozi, P. Eklund, J. Emmerlichc, H. HÖgberg, T. Meehan, P. Finkel, M.W. Barsoum, J.D. Hettinger, L. Hultman, S.E. Lofland, Solid State Commun. 146 (2008) 498.
[33] O.L. Anderson, J. Phys. Chem. Solids 24 (1963) 909.
[34] J.P. Poirier, Introduction to the Physics of the Earth's Interior, Cambridge University Press, Cambridge, UK, 2000.
[35] E. Francisco, J.M. Recio, M.A. Blanco, A. Martín Pendás, A. Costales, J. Phys. Chem. A 102 (1998) 1595.
[36] D.B. Sirdeshmukh, K.G. Subhadra, Phys. Stat. Sol. (b) 150 (1988) K11.
[37] H.Z. Fu, L.D. Hua, P. Feng, G. Tao, C.X. Lu, J. Alloys Compd. 473 (2009) 255.
[38] H.Z. Fu, L.D. Hua, P. Feng, G. Tao, C.X. Lu, Comput. Mater. Sci. 44 (2008) 774.
[39] H.Z. Fu, W.M. Peng, G. Tao, Mater. Chem. Phys. 115 (2009) 789.